

# Opioid Receptor Homo- and Heterodimerization in Living Cells by Quantitative Bioluminescence Resonance Energy Transfer

Danxin Wang, Xiaochun Sun, Laura M. Bohn, and Wolfgang Sadée

Department of Pharmacology, School of Medicine and Public Health, The Ohio State University, Columbus, Ohio

Received December 13, 2004; accepted March 11, 2005

## ABSTRACT

Opioid receptors have been shown to dimerize or oligomerize among themselves and each other, affecting their functional properties. This study used bioluminescence resonance energy transfer (BRET) between the  $\mu$ ,  $\delta$ , and  $\kappa$  opioid receptors to study opioid receptor aggregation in transfected human embryonic kidney 293 cells. Titration of receptor levels indicated that all three opioid receptors have a similar affinity to form homo- or hetero-oligomers in combination with any other opioid receptor type. In contrast, none of the opioid receptors formed detectable oligomers with the muscarinic M2 receptor, indicating that interactions among opioid receptors are selective. The formation of opioid receptor dimers, rather than higher

order oligomers, is supported by binding kinetics in competition experiments between labeled and unlabeled receptors. Opioid receptor dimerization occurred at physiological temperatures upon receptor biosynthesis, before trafficking to the plasma membrane. Moreover, using BRET, coimmunoprecipitation, receptor binding, and G protein coupling, we demonstrate for the first time functional  $\mu$  opioid receptor- $\kappa$  opioid receptor heterodimerization. These combined results demonstrate that opioid receptors can undergo homo- and heterodimerization, a process with potential implications for opioid physiology and pharmacology.

G protein-coupled receptors (GPCRs), the main targets for pharmacological agents, have been shown to form dimers or oligomers between identical receptors (homo-oligomerization) or different receptors (hetero-oligomerization) (Bouvier, 2001; George et al., 2002). First evidence of GPCR oligomerization came from coimmunoprecipitation of epitope-tagged receptors (Hebert et al., 1996; Cvejic and Devi, 1997; Jordan and Devi, 1999). This technique requires the lysis of cells with detergents at low temperature (4°C), a process that could disrupt lipid structure and cause nonspecific aggregation or fail to preserve transient or unstable interactions during the detergent treatment. Light resonance energy transfer techniques, such as fluorescence and bioluminescence resonance energy transfer (FRET and BRET) permit the monitoring of GPCR oligomerization in living cells (Angers et al., 2000) (Overton and Blumer, 2000). The con-

cept of GPCR oligomerization has prompted a revision of the traditional model of a signal transduction unit containing monomeric receptors coupling to single heterotrimeric G proteins and effector proteins.

The opioid receptors, belonging to the rhodopsin family of GPCRs,  $\mu$ ,  $\delta$ , and  $\kappa$  (MOR, DOR, and KOR), play pervasive roles in pain perception, locomotion, reward, autonomic function, immunomodulation, hormone secretion, and addiction. Several lines of evidence, including BRET and FRET analysis, suggest that opioid receptors form homo- and heterodimers/oligomers (Cvejic and Devi, 1997; Jordan and Devi, 1999; George et al., 2000; McVey et al., 2001; Ramsay et al., 2002). Oligomerization of opioid receptors has been suggested to play a role in receptor activation and internalization (Cvejic and Devi, 1997; He et al., 2002). Moreover, hetero-oligomerization of opioid receptors seems to generate novel ligand binding properties, in some cases resembling pharmacologically defined opioid receptor subtypes but not represented by unique genes (Jordan and Devi, 1999; George et al., 2000; Gomes et al., 2000). For example, the affinity of

This work was supported by National Institutes of Health grant DA04166. Article, publication date, and citation information can be found at <http://molpharm.aspetjournals.org>. doi:10.1124/mol.104.010272.

**ABBREVIATIONS:** GPCR, G protein coupled receptor; FRET, fluorescence resonance energy transfer; BRET, bioluminescence resonance energy transfer; MOR,  $\mu$  opioid receptor; DOR,  $\delta$  opioid receptor; KOR,  $\kappa$  opioid receptor; HEK, human embryonic kidney; GFP, green fluorescent protein; Rluc, *Renilla reniformis* luciferase; PCR, polymerase chain reaction; PBS, phosphate-buffered saline; BSA, bovine serum albumin; DAMGO, [D-Ala<sup>2</sup>, N-Me-Phe<sup>4</sup>, Gly<sup>5</sup>-ol]-enkephalin; GTP $\gamma$ S, guanosine 5'-O-(3-thio)triphosphate; SNC80, (+)-4-[( $\alpha$ R)- $\alpha$ -(2S,5R)-4-allyl-2,5-dimethyl-1-piperazinyl]-3-methoxybenzyl]-N,N-diethylbenzamide; BRL 52537, ( $\pm$ )-1-(3,4-dichlorophenyl)acetyl-2-(1-pyrrolidinyl)methylpiperidine; TM, transmembrane; U-69593, (+)-(5 $\alpha$ ,7 $\alpha$ ,8 $\beta$ )-N-methyl-N-[7-(1-pyrrolidinyl)-1-oxaspiro[4.5]dec-8-yl]benzeneacetamide; GR89696, 1-((3,4-dichlorophenyl)-acetyl)-4-acetyl-2-(1-pyrrolidinylmethyl)piperazine; CI-977, enadoline hydrochloride.

a MOR-DOR complex is similar to the proposed DOR<sub>2</sub> subtype, and a DOR-KOR complex to the KOR<sub>2</sub> subtype (Gomes et al., 2000; Jordan and Devi, 1999). Evidence from MOR knockout mice also suggests the involvement of MOR in DOR-mediated antinociception and receptor trafficking (Morinville et al., 2003). MOR-DOR interactions have also been supported by pharmacological studies in mice (Gomes et al., 2004).

All three opioid receptors seem to form homo-oligomers, whereas DOR/KOR and MOR/DOR form hetero-oligomers (Jordan and Devi, 1999; Gomes et al., 2000). Previous studies using immunoprecipitation failed to detect the interaction between MOR and KOR, and modeling studies also predicted that this interaction might not occur (Filizola et al., 2002). To further test this in living cells, we measured the interaction between MOR and KOR using BRET assay in the present study. Moreover, the relative affinity between each receptor subtype and the oligomerization state (e.g., dimer, trimer, tetramer) remained unknown. All three opioid receptors are expressed in spinal cord and can be colocalized in the same neuron (Ji et al., 1995). In cells coexpressing several receptors, the relative affinity between receptors determines which receptors are more likely to form homo- or heterodimers. In the present study, BRET was combined with analysis of receptor ligand binding for a quantitative evaluation of opioid receptor oligomerization in HEK-293 cells. Experiments with varying levels of labeled and unlabeled receptors served to estimate the relative affinity among each other and the oligomerization state. This revealed that opioid receptors form primarily dimers, with equal affinity among each other, including MOR-KOR. In addition, studies were performed to determine the subcellular location of opioid receptor dimers and the probable site of dimerization.

## Materials and Methods

**Materials.** GFP<sup>2</sup> and *Renilla reniformis* luciferase fusion protein expression vectors (GFP-N1 and Rluc-N1) were from PerkinElmer Life and Analytical Sciences (Torrance, CA). [<sup>3</sup>H]Diprenorphine (60 Ci/mmol) was from Amersham Biosciences Inc. (Piscataway, NJ). Coelenterazine H was from Molecular Probes (Eugene, OR). Deep Blue coelenterazine was from PerkinElmer Life and Analytical Sciences. Anti-GFP antibody was from BD Biosciences Clontech (Palo Alto, CA). Anti-FLAG monoclonal antibody (M2) was from Sigma-Aldrich (St. Louis, MO). Anti-c-Myc (9E10) antibody was from Santa Cruz Biotechnology Inc. (Santa Cruz, CA). Anti-Na/K-ATPase and anti-calnexin antibodies were from Abcam (Cambridge, MA). Materials for tissue culture were from Invitrogen (Carlsbad, CA). All other reagents were from Sigma-Aldrich or Fisher Scientific Co. (Fairlawn, NJ).

**Receptor Constructs.** The human *MOR*, mouse *DOR*, and human *KOR* coding sequences without their stop codon were amplified from the receptor expression plasmids using sense and antisense primers harboring unique cloning sites (HindIII and KpnI for *MOR* and *KOR*, and KpnI and BamHI for *DOR*). The PCR fragments were then inserted in-frame into both GFP-N1 and Rluc-N1 vectors to yield constructs named MOR-GFP, MOR-Rluc, DOR-GFP, DOR-Rluc, KOR-GFP, and KOR-Rluc. The sequences of all constructs were confirmed by DNA sequencing. To study whether opioid receptor nonspecifically heterodimerized with other G protein-coupled receptors, we also labeled human muscarinic M2 receptor with GFP- and Rluc using PCR methods.

**Cell Culture and Transfection.** HEK-293 cells were cultured in Dulbecco's modified Eagle's medium/Ham's F-12 50/50 (Fisher Sci-

entific Co.) supplemented with 10% fetal bovine serum, 100 units/ml penicillin, and 10 µg/ml streptomycin. For transfection, cells were seeded in six- or 12-well plate and cultured for 24 h. Transient transfections were performed using LipofectAMINE 2000 (Invitrogen) or metafectene (Biontex, Munich, Germany) according to the manufacturer's manual. To establish MOR-KOR-coexpressing stable cell lines, the same amounts of plasmids encoding N-terminal Myc-tagged rat *MOR* and FLAG-tagged human *KOR* (and equipped with different selection markers) were cotransfected into HEK-293 cells. Twenty-four hours after transfection, cells were cultured in the presence of 400 µg/ml G418 (Geneticin) and 300 µg/ml Zeocin. Surviving colonies were screened using [<sup>3</sup>H]diprenorphine binding assay. The expression of both MOR and KOR on cell surface of coexpressing cell lines was determined by enzyme-linked immunosorbent assay as described below.

**Confocal Microscopy.** Cells in 12-well plates were transfected with 1 µg of GFP fused opioid receptors. Twenty-four hours after transfection, cells were trypsinized and plated into glass bottom culture dishes (MatTek, Ashland, MA) at a density of  $0.5 \times 10^4$  and cultured for another 24 h. Living cells were observed using a laser scanning confocal microscope.

**BRET Assay.** HEK-293 cells were cotransfected with vectors expressing the GFP- and Rluc-fusion proteins in a ratio of 10:1. Twenty-four hours after transfection, cells were harvested and washed once with phosphate-buffered saline (PBS). The cells were then suspended in Dulbecco's PBS (PBS + 0.1% glucose + 0.01% CaCl<sub>2</sub> + 0.01% MgCl<sub>2</sub>), and distributed into 96-well microplates (white Optiplate; PerkinElmer Life and Analytical Sciences) at a density of 50,000 cells per well. DeepBlue C was added at a final concentration of 5 µM, and the readings at 410 and 515 nm were measured simultaneously using Fusion system (PerkinElmer Life and Analytical Sciences). The BRET signal was determined by the ratio of the light emitted by the receptor-GFP (515 nm) over the light emitted by the receptor-Rluc (410 nm). The background signal was determined by transfection of receptor-Rluc alone or receptor-Rluc plus GFP construct lacking the receptor sequence, which is less than 0.04 and was subtracted from total BRET signal.

**Fluorescent and Luminescent Activity Measurement.** Cells cotransfected with GFP- and Rluc-fusion proteins were distributed in 96-well microplates (white Optiplate) at a density of 50,000 cells per well. Total fluorescence of the cell suspensions was measured using Fusion system with an excitation filter at 410 nm, an emission filter at 515 nm, and the following parameters: read time 0.1 s, light source intensity 1, and high voltage 500. After the fluorescence measurement, the same cells were incubated for 10 min with coelenterazine H at a final concentration of 5 µM. Total cell luminescence was measured using Fusion system with the following parameters: read time 1 s and high voltage 600. Background fluorescence and luminescence were determined in wells containing untransfected cells.

**Correlation of Receptor Number with Fluorescent Intensity or Luciferase Activity.** HEK-293 cells were transfected with different amounts of plasmids encoding GFP- or Rluc-fused receptors in 12-well plates. Twenty-four hours after transfection, cells were collected and fluorescence and luminescence were measured as described above. The same cells were then collected, washed with buffer containing 50 mM Tris-HCl, pH 7.5, and 5 mM EDTA, and incubated with 2 nM [<sup>3</sup>H]diprenorphine in 500 µl of the same buffer at 23°C for 1 h. The reactions were stopped by rapid filtration through Whatman GF/C glass fiber filter. Nonspecific binding was determined in untransfected cells. Receptor densities are expressed in femtomoles of receptor per milligram of total cell proteins. The receptor density was plotted against fluorescent intensity or luciferase activity. Because the fluorescence or luminescence levels are intrinsic characteristics of each construct, the linear regression curve for each construct can be used to convert fluorescence or luminescence level into receptor densities.

**BRET Saturation Curves.** The experiments were performed as described by Mercier et al. (2002) with modifications. Cells in 12-well plates were cotransfected with a constant amount of Rluc-fused receptors (0.2  $\mu$ g for MOR, 0.1  $\mu$ g for DOR and KOR) and different amounts of GFP-fused receptors ( $\sim$ 0.1–2  $\mu$ g). Twenty-four hours after transfection, the cells were distributed into different 96-well microplates (white Optiplate) for BRET assay as described above. The same amount of cells from the same pool was also measured for fluorescent and luminescent intensity. The fluorescent and luminescent intensities were converted into receptor density using the GFP-receptor or Rluc-receptor linear regression curves (Fig. 2). The ratio of GFP-receptor density/Rluc-receptor density was plotted against the BRET signal (after subtracting background signal) to construct BRET saturation curves fitted with the Prism program.

**BRET Competition Assay.** Cells in 12-well plates were cotransfected with constant amounts of expression vectors encoding GFP- and Rluc-fusion receptors (*MOR-GFP/MOR-Rluc*, *DOR-GFP/DOR-Rluc*, and *KOR-GFP/KOR-Rluc*) at  $\sim$ 1:1 protein ratio, and in addition with increasing amounts of expression vectors for unlabeled wild-type MOR, DOR, and KOR, respectively. BRET ratios were measured 24 h after transfection. The same amount of cells from the same pool was also used to measure fluorescent intensity and luciferase activity as described above. The total amount of receptor expressed was determined by 2 nM [ $^3$ H]diprenorphine binding assay. The densities of GFP- or Rluc-fusion receptors were calculated from GFP-receptor or Rluc-receptor regression curves. The quantities of wild-type receptors were determined from the difference between total receptor amount and the sum of the Rluc- and GFP-fusion receptors. The ratio of competitor receptor (wild-type receptors)/BRET receptors (GFP- and Rluc-fused receptors) was plotted against the ratio of BRET signal in the presence of competitor versus BRET signal in the absence of competitor receptors (BRET/BRET<sub>0</sub>). The curves were fitted to binding models assuming the formation of dimers, trimers, or tetramers (Ayoub et al., 2002).

**Coimmunoprecipitation of Rluc-Fusion Receptors.** Cells in six-well plates were cotransfected with C-terminal GFP-fused receptors or N-terminal FLAG-tagged MOR, DOR, or KOR with Rluc-fusion receptors in a ratio of 1:1. Forty-eight hours after transfection, cells were washed with ice-cold PBS and lysed with buffer containing 50 mM Tris-HCl, pH 7.4, 300 mM NaCl, 10% glycerol, 1.5 mM CaCl<sub>2</sub>, 1 mM MgCl<sub>2</sub> plus protease inhibitors on ice for 30 min. The lysates were centrifuged at 27,000g for 10 min. The supernatants were incubated with anti-GFP or anti-FLAG antibodies for 2 h at 4°C. Then, 40  $\mu$ l of 50% protein A beads was added, and the mixture incubated for another hour at 4°C. The beads were washed three times with lysis buffer and then suspended in Dulbecco's PBS and distributed into 96-well microplates for luciferase activity assay using coelenterazine H. Nonspecific background was determined by cotransfection of GFP- or N-terminal-tagged receptors with Rluc construct without receptor fused or Rluc-fused muscarinic M2 receptor.

**Enzyme-Linked Immunosorbent Assay.** Cell surface receptors were determined by enzyme-linked immunosorbent assay as described previously (Lavoie et al., 2002). In brief, cells were cultured in polylysine-coated 12-well plate for 2 to 3 days, and then cells were washed three times with ice-cold PBS, blocked with 1% bovine serum albumin (BSA) in PBS for 30 min, and incubated with anti-Myc antibody (1:500) or anti-FLAG M2 antibody (1:1000) for 60 min. Cells were washed three times with 1% BSA in PBS and then fixed with 3% paraformaldehyde for 15 min followed by three washes with PBS. After blocking with 1% BSA in PBS for 15 min, cells were incubated with horseradish peroxidase-conjugated secondary antibody (1:1000) for 30 min, followed by three washes with PBS supplemented with 1% BSA and one wash with PBS. Tetramethylbenzidine peroxidase enzyme immunoassay substrate (Bio-Rad, Hercules, CA) were added to each well and incubated at room temperature for 30 min. After adding the same amount of 1 N H<sub>2</sub>PO<sub>4</sub>, the absorbance was read at 450 nm with a plate reader (Fusion system; PerkinElmer Life and

Analytical Sciences). Myc-MOR or FLAG-KOR individually expressing cell lines, expressed at different levels, served as controls to correct for the different affinity of two antibodies to their epitopes. In this manner, the approximate ratio of MOR and KOR expression level can be calculated from absorbance measurements in MOR-KOR-coexpressing cell line.

**Subcellular Fractionation.** Cells in 10-cm<sup>2</sup> dishes were cotransfected with GFP- and Rluc fused MOR, DOR, and KOR receptors in a ratio of 10:1. Forty-eight hours after transfection, cells were washed three times with ice-cold PBS buffer, harvested, and lysed with cold hypotonic lysis buffer (20 mM HEPES, pH 7.4, 2 mM EDTA, 2 mM EGTA, 6 mM MgCl<sub>2</sub>, 1 mM phenylmethylsulfonyl fluoride, and protease inhibitors). Cellular fractionation was performed as described by Terrillon et al. (2003) using discontinuous sucrose step gradient (0.5, 0.9, 1.2, 1.35, 1.5, and 2 M) and centrifugation at 130,000g for 16 h. In total, 31 fractions were obtained, and luminescence, fluorescence and BRET ratio were measured in 50  $\mu$ l of each sample. Fractions containing plasma membranes or endoplasmic reticulum were verified by immunoblotting using anti-Na/K-ATPase and anti-calnexin, to detect the respective cellular markers.

**Cell Membrane Preparation.** Stably transfected HEK-293 cells (Myc-tagged rat MOR, FLAG-tagged human KOR single expression cell lines, and Myc-tagged rat MOR and FLAG-tagged human KOR-coexpressing cell line) were cultured in 10-cm<sup>2</sup> dishes until confluent. Cells were washed once in ice-cold PBS and then homogenized in buffer containing 10 mM Tris-HCl, pH 7.4, and 0.1 mM EDTA, followed by centrifuging at 500g for 5 min. The supernatants were centrifuged at 40,000g for 15 min. The pellets were washed once with the same buffer and centrifuged again. The pellets from the second centrifugation were resuspended in homogenizing buffer, divided into aliquots, and stored at  $-70^{\circ}\text{C}$  until use.

**Radioligand Binding Assays and Ligand Competition Experiments.** Receptor binding assays were performed in buffer containing 50 mM Tris-HCl, pH 7.4, 5 mM EDTA, 20  $\mu$ g of membrane preparation, and different concentrations of [ $^3$ H]DAMGO, [ $^3$ H]U69593, and [ $^3$ H]diprenorphine at 23°C for 60 min. For ligand competition experiments, we used 0.5 nM [ $^3$ H]diprenorphine and different concentrations ( $\sim 10^{-11}$ – $10^{-4}$  M) of competing ligands as described by Jordan and Devi (1999). The reactions were stopped by rapid filtration over Whatman GF/C glass fiber filter. Specific binding was determined by total binding subtract nonspecific binding, which was determined in the presence of 10  $\mu$ M naloxone.

**[ $^{35}$ S]GTP $\gamma$ S Binding Assay.** GTP $\gamma$ S binding was performed in buffer containing 50 mM Tris-HCl, pH 7.4, 100 mM NaCl, 10 mM MgCl<sub>2</sub>, 1 mM EDTA, 0.1% BSA, 10  $\mu$ M GDP, 20  $\mu$ g of membrane, different concentrations of agonists, and 0.25 nM [ $^{35}$ S]GTP $\gamma$ S. The reaction mixtures were incubated at 30°C for 5 min. The reactions were stopped by adding 1 ml of ice-cold assay buffer, followed by centrifugation at 40,000g for 5 min. The pellets were washed once with PBS buffer. Then, scintillation cocktail was added to the tube and radioactivity was counted using scintillation counter.

**Statistical Analysis.** All curves were fitted using the Prism program. Data are expressed as means  $\pm$  S.E.M.

## Results

**BRET.** BRET is a protein-protein interaction assay based on energy transfer from a bioluminescent donor to a fluorescent acceptor protein. In this study, we used BRET<sup>2</sup> with DeepBlue C substrate, which emits blue light between 390 and 400 nm upon activation of *Renilla* luciferase. Stimulated at this wavelength, the GFP variant, GFP<sup>2</sup>, emits green light at 505 to 508 nm, when in molecular proximity to the Rluc, yielding large spectral resolution and high signal-to-noise ratio. The BRET<sup>2</sup> signal was measured as the ratio of green light emitted by GFP<sup>2</sup> over blue light emitted by Rluc. To



measure opioid receptor homo- or heterodimerization by BRET, we fused each receptor with GFP<sup>2</sup> or Rluc protein at the C terminus, generating all possible combinations. To test whether C-terminal tagging affects receptor function, we used the [<sup>35</sup>S]GTPγS binding assay to test agonist-stimulated response of fusion receptors in transiently transfected HEK-293 cell membranes. Shown in Table 1, the EC<sub>50</sub> values for specific agonists obtained from fusion receptor-transfected cells did not differ from that of wild-type receptors, indicating that C-terminal GFP or Rluc fusion did not affect receptor function, consistent with a previous report (Ramsay et al., 2002). We also used confocal microscopy to test the localization of GFP-tagged opioid receptors. The results show that GFP fused MOR, DOR, and KOR are localized in cell membrane (Fig. 1). Subcellular fractionation studies also indicate that the majority of GFP and Rluc activities were found in plasma membrane fractions (Fig. 6; see below) compared with endoplasmic reticulum.

**Relationship between Bioluminescent/Fluorescent Intensity and Receptor Density.** For quantitative BRET measurements, the expression level of both the donor and acceptor protein in cotransfected cells must be known. Because the fluorescent intensity and luciferase activity are intrinsic characteristics of each fusion protein, the expression level can be determined by fluorescent intensity or luciferase activity. We constructed titration curves for GFP fluorescence intensity or luciferase activity versus receptor density (measured with [<sup>3</sup>H]diprenorphine; femtomoles per milligram) for each receptor (Fig. 2). The receptor expression levels were linearly related to both fluorescent intensity and luciferase activity. These curves subsequently served for converting fluorescent intensity or luciferase activity into receptor density (femtomoles per milligram).

**BRET Saturation Curves.** With a fixed amount of donor receptor (MOR-Rluc, DOR-Rluc, and KOR-Rluc at ~100 fmol/mg of protein, monitored by luciferase activity), the BRET signal increased when the level of acceptor receptor (MOR-GFP, DOR-GFP, and KOR-GFP) increased (from ~50 to ~1500 fmol/mg of protein, monitored by fluorescence intensity) and reached a maximum level (Fig. 3). The ratio of acceptor/donor required to reach 50% maximum BRET ratio is assumed to represent the affinity of donor-acceptor interaction (Mercier et al., 2002). Shown in Table 2, maximum BRET signals (BRET<sub>max</sub>) induced by different pairs of acceptor and donor receptors vary considerably, with DOR-DOR interactions yielding the largest BRET<sub>max</sub> signal. BRET yield

is not only determined by the number of receptor oligomers formed but also by the distance between the Rluc donor and GFP acceptor. Therefore, the difference in BRET<sub>max</sub> could result from different orientations of Rluc- and GFP in the oligomerized fusion proteins. In hetero-oligomerization experiments, switching of donor (Rluc) and acceptor (GFP) receptors did not significantly affect BRET<sub>50</sub> but changed BRET<sub>max</sub> values (Table 2), demonstrating the contribution of different Rluc and GFP orientations in the fusion proteins. However, the ratio of acceptor/donor to attain 50% of the maximum BRET signal (BRET<sub>50</sub>) did not significantly differ among different pairs of opioid receptors. This result indicates that the affinities of all possible pairs of the three opioid receptors are similar, suggesting that different opioid receptors have similar propensity to form homo- and hetero-oligomers if coexpressed in the same cell. Stimulation of MOR, DOR, and KOR with the selective agonists DAMGO, SNC80, and BRL 52537 (10 μM; 10 min), respectively, had no effect on BRET<sub>50</sub> and BRET<sub>max</sub> for MOR, DOR, or KOR homo-oligomerization (Table 2), indicating agonist stimulation does not change the distance between the receptor labels because opioid receptor homo-oligomers seem to be constitutively formed.

To rule out the possibility that the BRET signal is caused by nonspecific aggregation of membrane receptors, we also tagged human muscarinic M2 receptors with both GFP- and Rluc, and measured BRET signal between M2-M2 and M2-opioid receptors. Shown in Fig. 4, when cells were cotransfected with M2-GFP and M2-Rluc, a significant BRET signal was observed, indicating homodimerization of M2 receptor, consistent with immunoprecipitation result using different epitope-tagged M2 receptor (Park and Wells, 2003). However, when cells were cotransfected with GFP- or Rluc-fused M2 and any Rluc- or GFP-tagged opioid receptor, BRET ratios were not significantly different from that of background (determined by cotransfection of any GFP-fused receptor and Rluc alone). This result indicates that opioid receptors do not interact with the M2 receptor and further implies that the opioid receptor interactions are selective. In each case, the expression levels of Rluc- and GFP-fusion receptors were ~100 to 200 and ~1000 to 2000 fmol/mg of protein, respectively, tested by [<sup>3</sup>H]diprenorphine (for opioid receptor) and [<sup>3</sup>H]methylscopolamine (for M2 receptor) binding assay. Under this condition, GFP/Rluc ratio is ~10:1, leading to maximum BRET ratios for opioid receptor interactions (Fig. 3). Moreover, with a constant amount (~100 fmol/mg of protein) of MOR-Rluc, DOR-Rluc, or KOR-Rluc combined with increasing amounts of M2-GFP (from ~50 fmol to ~1.3 pmol/mg of protein), no BRET signal was observed for M2-GFP combined with any opioid receptor, in contrast to the robust BRET signal observed for opioid receptor interactions (Fig. 3).

**Effect of Temperature on Receptor Oligomerization.** Lipid-receptor interactions are important for maintaining the conformation of membrane receptors and may be altered at low temperatures in mammalian cells (Chabre et al., 2003; Fotiadis et al., 2003). Therefore, we measured BRET signals both at room temperature (23°C) and at 37°C. Shown in Fig. 3, BRET saturation curves performed at 37°C did not differ from those at room temperature, with similar BRET<sub>50</sub> and BRET<sub>max</sub> values (Table 2). This result indicates that BRET

TABLE 1

EC<sub>50</sub> values for opioid agonists, DAMGO, DPDPE, and U69593 obtained from [<sup>35</sup>S]GTPγS binding dose-response curves performed in wild-type or GFP/Rluc-fused opioid receptor transfected HEK cell membranes

Data presented as mean ± S.E.; n = 3.

Receptor	DAMGO	DPDPE	U69593
hMOR	27 ± 15	N.D.	N.D.
hMOR-GFP	12 ± 11	N.D.	N.D.
hMOR-Rluc	18 ± 14	N.D.	N.D.
mDOR	N.D.	2.6 ± 1.2	N.D.
mDOR-GFP	N.D.	1.7 ± 1.3	N.D.
mDOR-Rluc	N.D.	4.4 ± 1.3	N.D.
hKOR	N.D.	N.D.	3.6 ± 2.1
hKOR-GFP	N.D.	N.D.	1.2 ± 1.5
hKOR-Rluc	N.D.	N.D.	1.8 ± 1.8

DPDPE, [D-Pen<sup>2</sup>, D-Pen<sup>5</sup>]-enkephalin; N.D., not determined.

signals detected at room temperature are not an artifact of lipid phase transitions.

**Oligomerization State of Opioid Receptors.** We used competition curves between unlabeled and labeled opioid receptors using BRET signals to assess opioid receptor homo-oligomerization states as described by Ayoub et al. (2002). The BRET signal decreased with increasing levels of competing unlabeled receptors (wild-type receptor without GFP or Rluc labeling) (Fig. 5). Fitting the results to a dimer, trimer, or tetramer model, the data from MOR-MOR, DOR-DOR, and KOR-KOR interactions were best accounted for by receptor dimer formation (Fig. 5;  $r^2 = 0.9536$  for MOR;  $r^2 = 0.9597$  for DOR and  $r^2 = 0.9517$  for KOR). This result indicates that opioid receptor interactions are mostly dimeric, or dimerization is the primary building block for opioid receptor oligomerization detectable by BRET. In contrast, cotransfection of unlabeled M2 receptor did not affect BRET signal for any of three opioid receptor interactions, indicating the inhibition by unlabeled opioid receptors is specific (Fig. 5).

**Subcellular Distribution of Opioid Receptor Homodimers.** We performed BRET assay in subcellular fractions obtained from ultracentrifugation of cell membranes on a sucrose gradient (Terrillon et al., 2003). This method produces plasma membranes in fractions 7 to 15 and endoplasmic reticulum in fractions 19 to 27 (Terrillon et al., 2003; Salahpour et al., 2004). This was confirmed by immunoblotting using the plasma membrane and endoplasmic reticulum markers Na/K-ATPase and calnexin, respectively (Fig. 6d). Two peaks of luminescence and fluorescence activity were observed in all three opioid receptor transfected cell preparations, with the major peak (>70% total activity) seen in fractions corresponding to plasma membranes, and the minor peak (~20% of total activity) to endoplasmic reticulum (Fig. 6), indicating that the majority of GFP- and Rluc-fused opioid receptors resided in the plasma membrane. BRET signals were detectable in both plasma membrane and endoplasmic reticulum fractions, suggesting that opioid receptor dimerization can occur before receptors are transported to the cell surface.

To determine whether dimerization occurs before plasma membrane transport, we transfected HEK-293 cells stably expressing unlabeled individual opioid receptor (at densities of 1.7, 1.5, and 1.8 pmol/mg of protein for MOR, DOR, and KOR, respectively) with the corresponding GFP- and Rluc-labeled receptors. If dimerization or equilibration were to occur after transport to the plasma membrane, unlabeled receptors would have been expected to compete with tagged receptors, resulting in a decreased BRET signal. Shown in Fig. 7a, BRET signals obtained from wild-type HEK-293 cells

did not differ from those obtained in cell lines stably expressing unlabeled opioid receptors. In a corollary experiment, cell lines stably expressing MOR-GFP, DOR-GFP, or KOR-GFP were transiently transfected with Rluc-fused opioid receptors. Again, no significant BRET signals were observed (Fig. 7b). Together, these results demonstrate that opioid receptor dimerization occurs before the receptor has been transported to the cell membrane; moreover, receptor dimers are stable and do not equilibrate with other receptors once formed.

**Relationship between Receptor Expression Level and BRET Signal.** To test whether protein interactions occur at physiological expression levels, we cotransfected different concentration of GFP- and Rluc-fused opioid receptors yielding expression levels ranging from ~100 to ~5000 fmol/mg of protein (Fig. 8). When the GFP/Rluc ratio is >10 (saturation of BRET signals; Fig. 3), the BRET signals (expressed as a ratio) are similar for every pair of opioid receptors regardless of receptor expression level, which was as low as ~100 fmol/mg of protein (Fig. 8).

**Coimmunoprecipitation of Rluc Fusion Receptors.** Hetero-oligomerization of DOR-KOR and MOR-DOR had been reported, whereas the interaction between MOR and KOR was uncertain. Jordan and Devi (1999) were unable to show interaction between MOR-KOR by coimmunoprecipitation of differently epitope-tagged MOR and KOR. In the present study, we detected a robust interaction between MOR and KOR using the BRET assay. To test MOR-KOR heterodimer formation further, we performed coimmunoprecipitation of GFP-fused receptors with Rluc-fused receptors, followed by Rluc activity measurement. Rluc without a fused receptor and Rluc-tagged M2 receptors served as background controls. Shown in Fig. 9a, Rluc-fused MOR, DOR, and KOR coimmunoprecipitated with GFP-fused MOR, DOR, and KOR in each combination, whereas no Rluc activity was recovered with the Rluc construct alone or with fused muscarinic M2 receptor. Similar results were obtained when using N-terminally FLAG-tagged MOR, DOR, and KOR instead of the GFP fusion proteins (Fig. 9b), indicating that the tags did not interfere. The interaction between MOR-KOR did not differ from other receptor interactions, supporting direct physical interaction between MOR and KOR.

**Radioligand Binding Assay.** To characterize the pharmacological properties of MOR-KOR heterodimers, we established a cell line stably coexpressing N-terminal Myc-tagged rat MOR and FLAG-tagged human KOR, with 1.5 pmol/mg total opioid receptors (2 nM [<sup>3</sup>H]diprenorphine binding in whole cell) and a cell surface MOR/KOR ratio of ~0.8/1 (measuring Myc-tag or FLAG-tag immunoreactivity by enzyme-linked immunosorbent assay; for details, see *Materials*

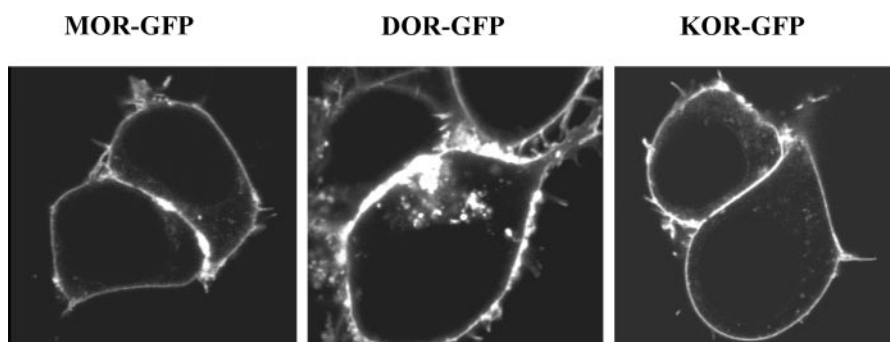


**Fig. 1.** Confocal microscope image of HEK-293 cells expressing MOR-GFP, DOR-GFP, and KOR-GFP. HEK-293 cells were transiently transfected with plasmids encoding MOR-GFP, DOR-GFP, and KOR-GFP. Forty-eight hours after transfection, images were taken in living cells using confocal microscopy.

and Methods). Stably transfected cell lines expressing only MOR or KOR served as controls, expressing Myc-tagged MOR at 0.75 pmol/mg and FLAG-tagged KOR at ~0.7 pmol/mg densities (whole cell [ $^3\text{H}$ ]diprenorphine binding). We first performed [ $^3\text{H}$ ]DAMGO, [ $^3\text{H}$ ]U69593, and [ $^3\text{H}$ ]diprenorphine saturation binding assays in cell membranes obtained from these cell lines (Table 3). Compared with MOR and KOR, MOR-KOR has ~5 times lower binding affinity for MOR-specific ligand [ $^3\text{H}$ ]DAMGO ( $P < 0.01$ ), and similar binding affinity for the KOR-specific ligand [ $^3\text{H}$ ]U69593 and a nonspecific opioid ligand [ $^3\text{H}$ ]diprenorphine. To test possible dimerization effects further, we used 0.5 nM [ $^3\text{H}$ ]diprenorphine as a tracer and determined competitive inhibition by unlabeled MOR- and KOR-specific agonists as described for DOR-KOR heterodimer (Jordan and Devi, 1999) (Table 4). Consistent with the [ $^3\text{H}$ ]DAMGO binding assay, high-affinity binding sites for DAMGO were undetectable in MOR-KOR-coexpressing cell membranes. This seems to be a specific effect, because DAMGO maintains high affinity to a portion of sites in a mixture of membranes from cells individually expressing MOR and KOR (MOR + KOR, in a 1:1 ratio) (Table 4). Similar results were obtained with the MOR-specific agonist endomorphin-1 (Table 4). In contrast, the KOR-specific agonists U50488H and U69593, and the putative KOR<sub>2</sub> subtype-specific agonist GR89696 (Caudle et al., 1997; Ho et al., 1997; Eliav et al., 1999), have similar

binding affinities in membranes from cells expressing KOR alone or MOR-KOR (Table 4). Because cell surface labeling indicated that MOR-KOR-coexpressing cells did express MOR at a density of ~600 fmol/mg of protein (40% of total receptor density), these results suggest that the MOR-KOR heterodimer formation caused a loss of high-affinity binding sites for the MOR-specific agonists tested in this study.

**[ $^{35}\text{S}$ ]GTP $\gamma\text{S}$  Binding Assay.** To test G protein coupling of the MOR-KOR heterodimer, we observed the effects of different agonists on GTP $\gamma\text{S}$  binding in membranes from MOR-KOR-coexpressing cells. This was compared with the results

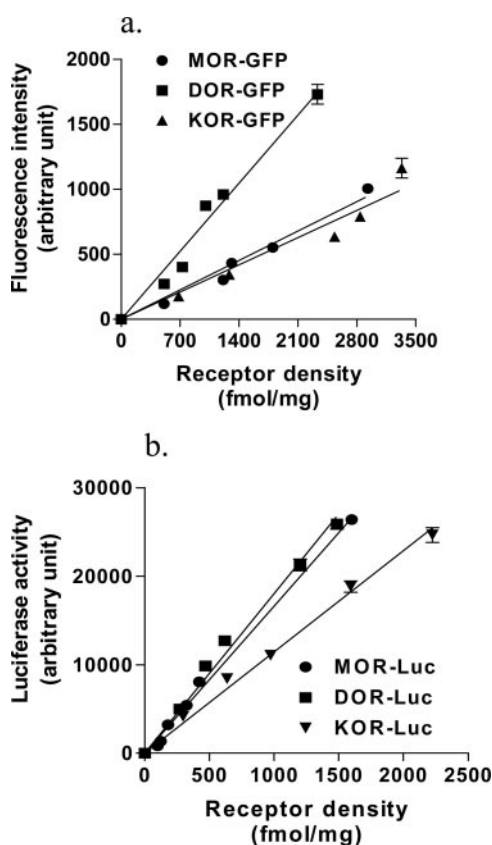


**Fig. 2.** Correlation of fluorescent intensity or luciferase activity with levels of receptor expression. HEK-293 cells were transfected with different doses of plasmids encoding GFP-fused MOR, DOR, or KOR (a) or Rluc-fused MOR, DOR, or KOR (b). Twenty-four hours after transfection, fluorescent intensity or luciferase activity as well as the number of diprenorphine binding sites were measured as described under *Materials and Methods*. Mean  $\pm$  S.E.M.,  $n = 3$  in duplicate.

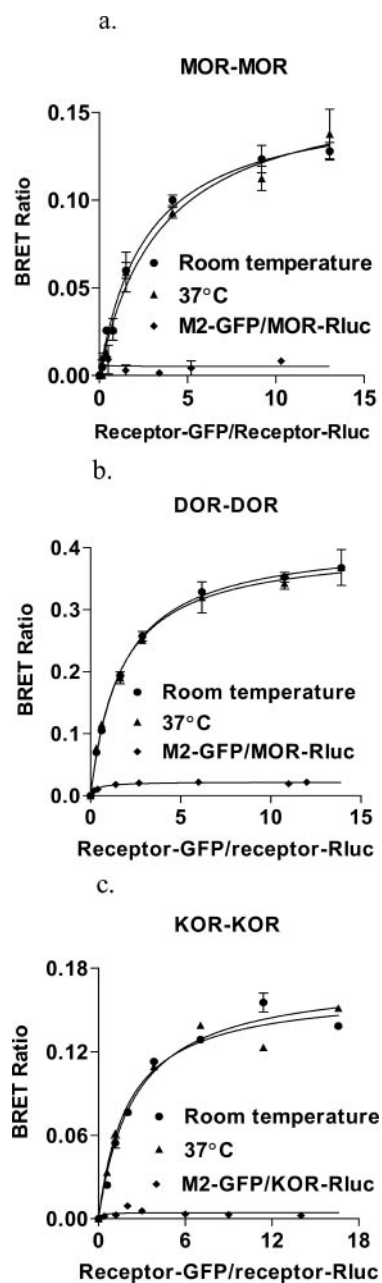


**Fig. 3.** BRET saturation curves for MOR (a), DOR (b), and KOR (c) homodimerization performed at room temperature or at 37°C. HEK-293 cells were cotransfected with a fixing dose of Rluc-fusion receptor construct and increasing doses of GFP-fusion receptor construct as described under *Materials and Methods*. Twenty-four hours after transfection, BRET signals were measured at room temperature or at 37°C. Cotransfection of M2-GFP with MOR-, DOR-, or KOR-Rluc did not induce any BRET signal (diamonds). Mean  $\pm$  S.E.M.;  $n = 3$  in duplicate.



from cells expressing only MOR or KOR, or their membrane mixtures. DAMGO dose dependently increased GTP $\gamma$ S binding in membranes from MOR-expressing cells and in MOR + KOR mixed membranes with similar EC<sub>50</sub> values (Table 5). The EC<sub>50</sub> values are similar to published results (Zhao et al., 2003; Shaqura et al., 2004). DAMGO also dose dependently increased GTP $\gamma$ S binding in membranes from MOR-KOR cells, but with 4-fold higher EC<sub>50</sub> value than that in MOR membrane or MOR + KOR mixed membranes ( $P < 0.05$ ) (Table 5), consistent with a lower affinity of MOR-KOR heterodimers for DAMGO (Tables 3 and 4). Because MOR and KOR expression levels in MOR-KOR membranes were similar to that in MOR + KOR mixed membranes, the different effects of DAMGO seem to result from direct MOR-KOR

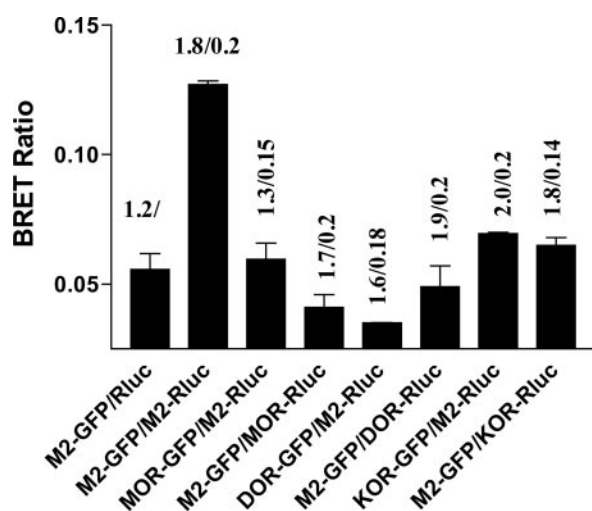
interactions. The shift in EC<sub>50</sub> obtained in the GTP $\gamma$ S binding assay for the MOR-KOR heterodimer is considerably smaller than the IC<sub>50</sub> shift obtained with [<sup>3</sup>H]diprenorphine binding (3-fold in GTP $\gamma$ S binding versus 24-fold in [<sup>3</sup>H]diprenorphine binding). Likewise, DAMGO also increased

TABLE 2

Receptor interaction parameters obtained from BRET saturation curves performed at room temperature (RT) or at 37°C, in the absence of agonist, or 10 min after agonist stimulation (10  $\mu$ M)

BRET<sub>max</sub> is the maximum BRET signal and BRET<sub>50</sub> represents the ratio of the density (femtomoles per milligram) of acceptor and donor receptors (acceptor/donor) yielding 50% maximum BRET signal. Data presented as mean  $\pm$  S.E.M.;  $n = 3$ , each measured in duplicate.

Acceptor/Donor	Interactions	BRET <sub>max</sub>	BRET <sub>50</sub>
MOR-GFP/MOR-Rluc	MOR-MOR		
	RT	0.16 $\pm$ 0.01	2.7 $\pm$ 0.5
	37°C	0.17 $\pm$ 0.01	3.5 $\pm$ 0.6
DOR-GFP/DOR-Rluc	DOR-DOR		
	RT	0.42 $\pm$ 0.01	1.8 $\pm$ 0.1
	37°C	0.40 $\pm$ 0.01	1.7 $\pm$ 0.2
KOR-GFP/KOR-Rluc	KOR-KOR		
	RT	0.18 $\pm$ 0.01	2.5 $\pm$ 0.2
	37°C	0.16 $\pm$ 0.01	2.0 $\pm$ 0.2
MOR-GFP/DOR-Rluc	MOR-DOR, RT	0.34 $\pm$ 0.01	3.7 $\pm$ 0.2
	MOR-DOR, 37°C	0.12 $\pm$ 0.01	3.2 $\pm$ 0.5
	MOR-DOR, 37°C + SNC80	0.41 $\pm$ 0.02	1.6 $\pm$ 0.1
MOR-GFP/KOR-Rluc	MOR-KOR, RT	0.14 $\pm$ 0.02	2.4 $\pm$ 0.7
	MOR-KOR, 37°C	0.22 $\pm$ 0.01	3.8 $\pm$ 0.6
	MOR-KOR, 37°C + BRL 52537	0.17 $\pm$ 0.01	2.1 $\pm$ 0.3
DOR-GFP/KOR-Rluc	DOR-KOR, RT	0.18 $\pm$ 0.01	2.5 $\pm$ 0.3
	DOR-KOR, 37°C	0.27 $\pm$ 0.01	1.8 $\pm$ 0.2
	DOR-KOR, 37°C + BRL 52537	0.17 $\pm$ 0.01	2.1 $\pm$ 0.3



**Fig. 4.** No significant BRET signals were observed with muscarinic M2 receptor (another G protein-coupled receptor) and opioid receptors. HEK-293 cells were cotransfected with GFP- and Rluc-fused receptor constructs as indicated at the ratio of 10:1. BRET ratios were measured 24 h after transfection. The numbers above the bars represent the density (picomoles per milligram) of GFP/Rluc fusion receptors tested by receptor binding assay as described under *Materials and Methods*. Means  $\pm$  S.E.M.;  $n = 3$ .

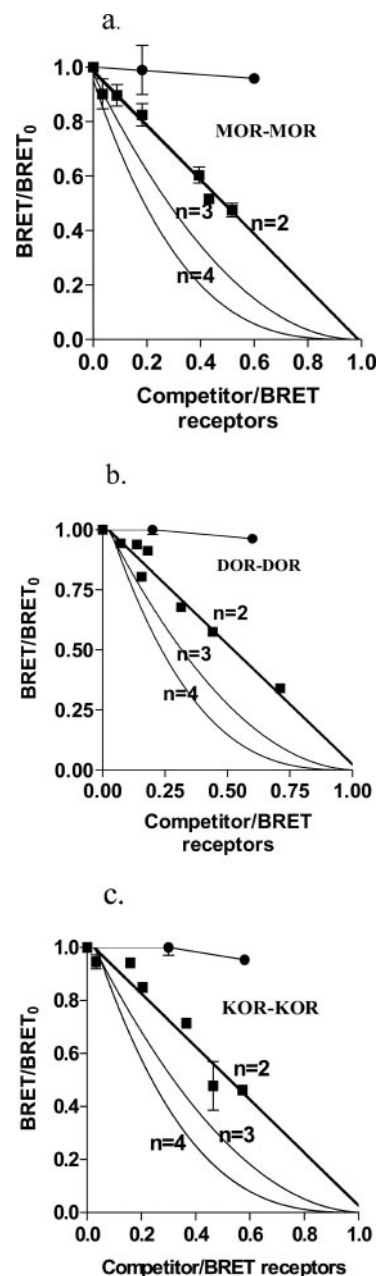


**Fig. 5.** BRET competition curves for MOR (a), DOR (b), and KOR (c) homodimerization. HEK-293 cells were cotransfected with a constant amount of paired fusion receptors (MOR-Rluc/MOR-GFP, DOR-Rluc/DOR-GFP, or KOR-Rluc/KOR-GFP, each expressed at 1:1 protein ratio) and increasing amounts of unlabeled wild-type MOR, DOR, KOR, or M2, respectively. Twenty-four hours after transfection, BRET signals and receptor expression levels were measured. Experimental data (■) are fitted to oligomerization models assuming formation of dimers, trimers, and tetramers model (Ayoub et al., 2002). For all three opioid receptors, best fits were obtained with the dimer model (bold curve,  $r = 0.9536$  for MOR;  $r = 0.9597$  for DOR; and  $r = 0.9517$  for KOR). Mean  $\pm$  S.E.M.;  $n = 3$  in duplicate. Competitor receptor: the wild-type receptors; BRET receptors: GFP- and Rluc-fused receptors; BRET/BRET<sub>0</sub>, the ratio of BRET signal in the presence of different concentrations of competitor receptor over that in the absence of competitor receptors. No competition was seen with wild-type M2 receptor cotransfection (●).

GTP $\gamma$ S binding in KOR membranes with EC<sub>50</sub> of 2.4  $\mu$ M (Table 5) as reported by Zhao et al. (2003), although DAMGO was unable to replace [<sup>3</sup>H]diprenorphine binding on KOR at 5  $\mu$ M (data not shown). This result indicates that GTP $\gamma$ S binding is a more sensitive assay than radioligand binding, capable of detecting weak functional interactions. In contrast, the KOR-specific agonists U69593, U50488H, and GR89696 have similar effects in cell membranes expressing KOR alone and MOR-KOR (Table 5). Other nonspecific agonists, morphine, dynorphin A1-13, etorphine, and bremazocine, also have similar effects in membranes from MOR-KOR-coexpressing cells and MOR or KOR singly expressing cells, or in mixed membranes of MOR and KOR cells (Table 5). The maximum effects induced by all agonists, ranging from 150 to 250% of basal binding, did not differ substantially between MOR-KOR-coexpressing membranes and MOR + KOR mixed membranes (data not shown).

## Discussion

In this study, we take advantage of quantitative features of BRET analysis, in combination with quantitative radioligand binding assays, to study homo- and heterodimerization of opioid receptors in transfected HEK-293 cells. The results

demonstrate that among MOR, DOR, and KOR, any of the possible receptor pairs has similar propensity for forming homo- and heterodimers. This suggests that in a coexpressing cell, homodimers and heterodimers can coexist in proportion to expression levels of the individual receptors.

Computational opioid receptor models suggest that transmembrane domains are important for opioid receptor homodimerization (Filizola and Weinstein, 2002). TM1 and TM4 are proposed to be responsible for MOR-MOR interaction, TM4 and TM5 for DOR, and TM5 for KOR homo-dimerization. These TM domains are highly conserved among the three opioid receptors (amino acid identity 70–90%). This might account for similar affinity for the interaction among the three opioid receptors. Furthermore, protein-protein interactions are favored over protein-lipid interactions in the membrane bilayer on thermodynamic grounds (Schneider et al., 2002), indicating that nonspecific interactions could contribute to dimerization.

Dimerization of rhodopsin, a related GPCR, observed by Foliadis et al. (2003) using atomic force microscopy, has been challenged (Chabre et al., 2003). Traditional biophysical techniques have defined rhodopsin as a monomeric receptor protein randomly dispersed and freely diffusing in a fluid

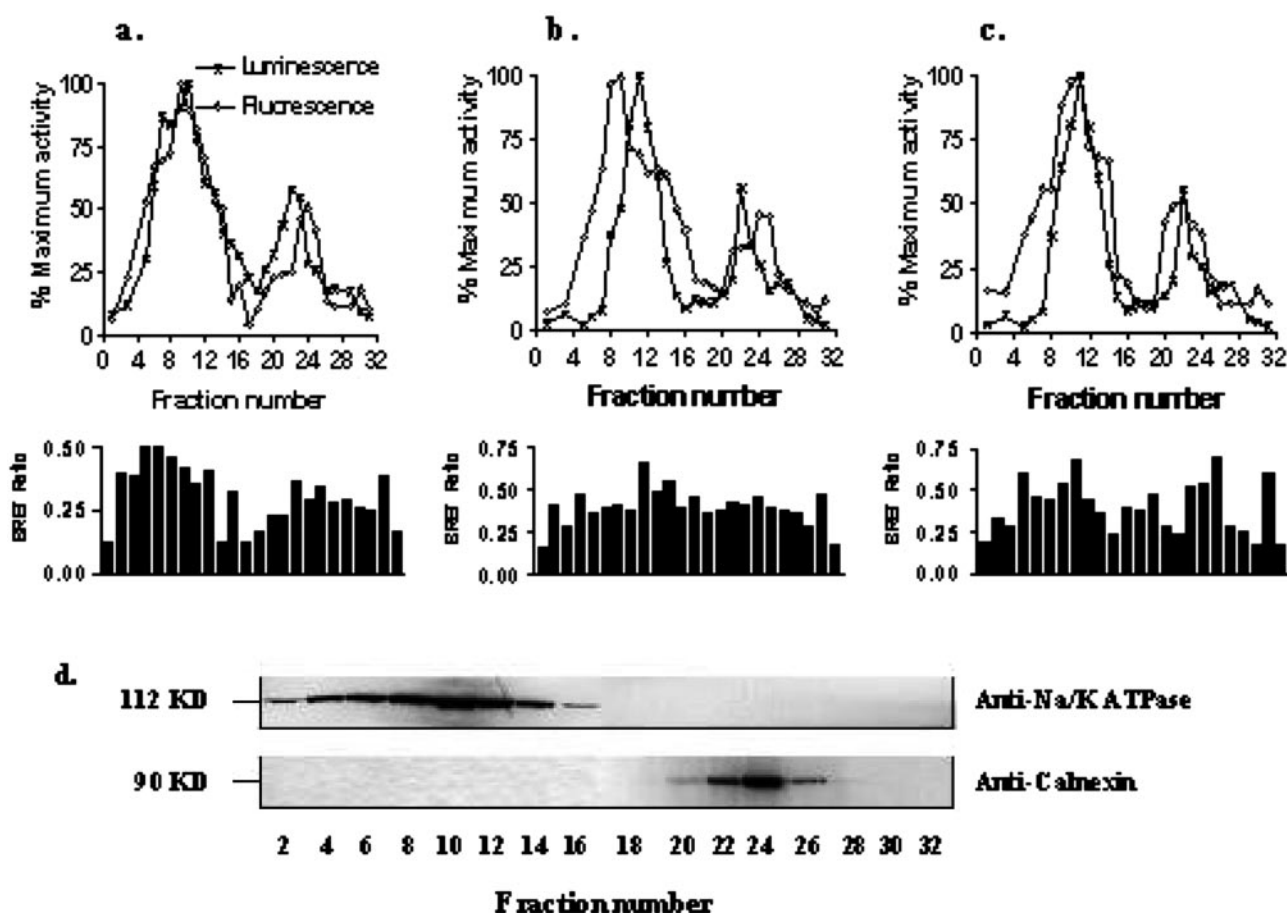


**Fig. 6.** Subcellular distribution of GFP- and Rluc-fused MOR (a), DOR (b), and KOR (c) opioid receptors and their dimers. HEK-293 cells transfected with GFP- and Rluc-fused receptor pairs (in a ratio of 10:1) were lysed, cell lysates applied to the top of a discontinuous sucrose gradient and centrifuged for 16 h at 130,000g. Fractions were subjected to fluorescence and luminescence analyses and to BRET measurements. Data are the means of two experiments. d, detection of Na/K ATPase (plasma membrane marker) and calnexin (endoplasmic reticulum marker) by Western blotting. Samples from MOR, DOR, or KOR transfection experiments were combined. Ten micrograms of protein from different fractions was loaded to a 8% SDS-PAGE, followed by Western blotting using anti-Na/K ATPase and anti-calnexin antibodies. The experiments are repeated twice with similar results.



lipid matrix in the rod-disc membrane, but sample preparation for atomic force microscopy excludes lipids from rhodopsin and causes protein aggregation (Chabre et al., 2003). Moreover, most previous studies were done at 25°C resulting in lipid phase separation with possible effects on protein aggregation (Chabre et al., 2003; Fotiadis et al., 2003). Yet, in the present study, BRET signals were similar at room temperature and at 37°C, indicating that opioid receptor dimerization occurs at physiological temperatures. Agonist stimulation had no effect on BRET signals under any condition tested, suggesting that oligomerization occurs constitutively. Furthermore, we demonstrate that these interactions occur at different levels of expression arguing against nonspecific interactions resulting from artifacts of overexpression systems.

Recent studies indicate that receptors can form higher order protein networks, yielding large protein arrays (Tucker et al., 2001). On SDS-PAGE gels, opioid receptors were seen

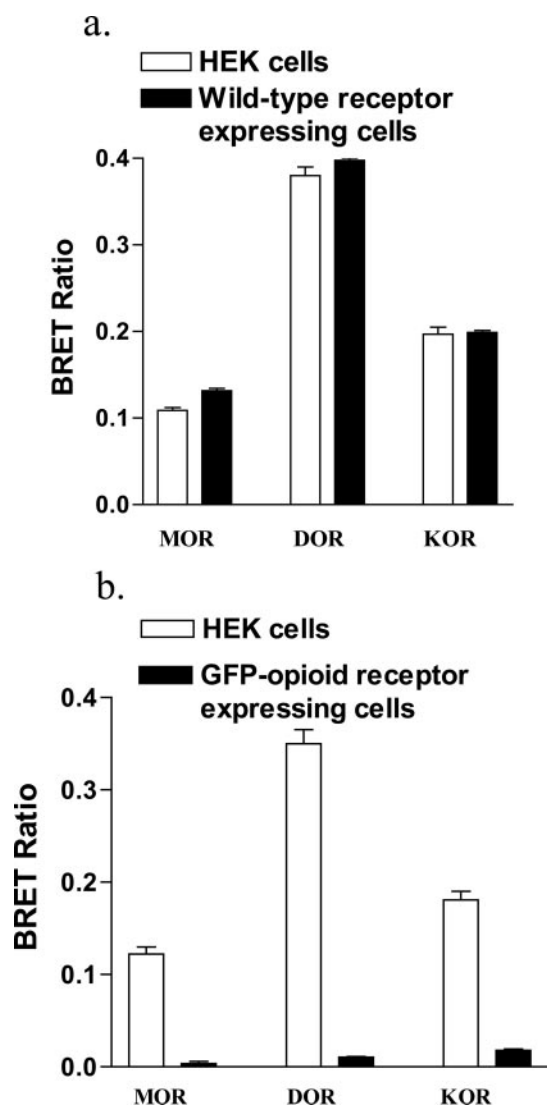


**Fig. 7.** a, effects of preexisting cell membrane untagged opioid receptor on BRET signal. HEK-293 cells or wild-type opioid receptors expressing HEK-293 cells were cotransfected with GFP- and Rluc-fused opioid receptor pairs. BRET ratios were measured 24 h after transfection. b, BRET assays in GFP-opioid receptor-expressing stable cell lines. HEK-293 cells stably expressing MOR-GFP, DOR-GFP, or KOR-GFP receptor were transfected with corresponding Rluc-fused opioid receptor, and BRET ratio measured 24 h after transfection (filled columns). As a control, HEK-293 cells were cotransfected with GFP- and Rluc-fused opioid receptor pairs (open columns). The expression levels of GFP- and Rluc-fused receptors are similar in two conditions. Mean  $\pm$  S.E.M.;  $n = 3$ .

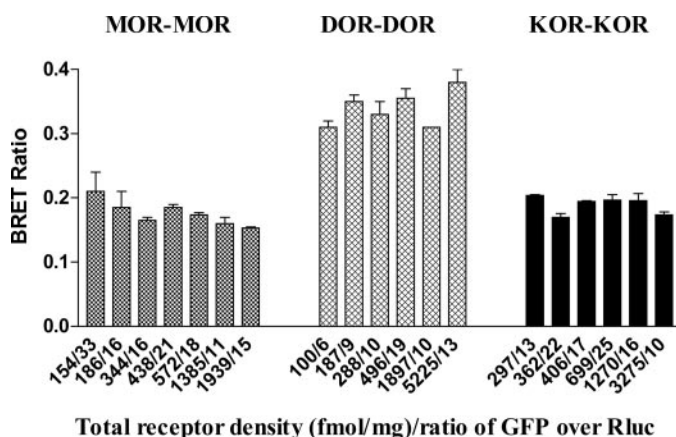


**Fig. 8.** Effects of receptor expression level on BRET signal. HEK-293 cells were cotransfected with different amounts of GFP- and Rluc-fused opioid receptor pairs. Twenty-four hours after transfection, luminescence/fluorescence and BRET ratio were measured. Receptor densities were calculated from luminescence/fluorescence intensity correction curves (Fig. 2). Mean  $\pm$  S.E.M.;  $n = 3$ . Numbers under each bar represent the receptors density (left, femtomoles per milligram) and the ratio of GFP/Rluc (right).

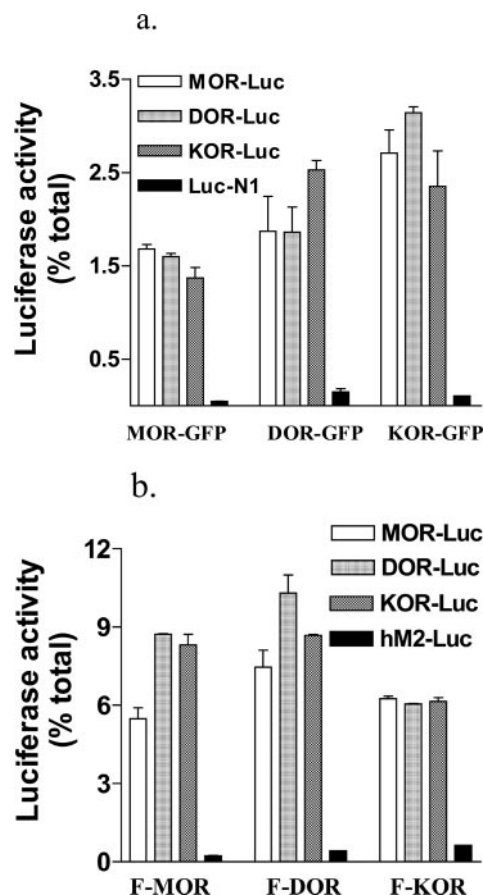


**Fig. 9.** Coimmunoprecipitation of GFP-fusion receptors (a) or FLAG-tagged receptors (b) with Rluc-fusion receptors. HEK-293 cells coexpressing Rluc fusion opioid receptors and GFP-fusion or N-terminal FLAG-tagged receptors were lysed and immunoprecipitated with anti-GFP or anti-FLAG antibody, respectively. Luciferase activity was measured in the precipitates. Values are presented as percentage of total luciferase activity in the cell lysates. Mean  $\pm$  S.E.M.;  $n = 3$  in duplicate.

Our results indicate that MOR-KOR can also form heterodimers with a similar affinity to that of MOR-DOR or DOR-KOR (Table 2). Coimmunoprecipitation of GFP-fused or FLAG-tagged MOR or KOR with Rluc-fused KOR or MOR

Although molecular cloning only revealed one KOR gene, pharmacological evidence had suggested the existence of

Data presented as mean  $\pm$  S.E.M.;  $n = 3$ . Where only partial displacement occurs, the residual tracer binding was subtracted to calculate  $IC_{50}$  values for the displaceable portion of tracer binding.

Compound	MOR-KOR	MOR + KOR	MOR	KOR
	<i>nM</i>			
DAMGO	>3000	110 ± 36	123 ± 43	>5000
Endomorphine-1	>1000	109 ± 28	116 ± 31	>2000
U69593	191 ± 82	137 ± 54	>1000	116 ± 79
U50488H	70 ± 8	54 ± 8	>1000	94 ± 8
GR89696	0.6 ± 0.1	0.6 ± 0.1	29 ± 7	0.2 ± 0.1

Binding parameters obtained from [<sup>3</sup>H]DAMGO, [<sup>3</sup>H]U69593, and [<sup>3</sup>H]diprenorphine saturation binding curves performed in MOR, KOR single expressing-, and MOR-KOR-coexpressing cell membranes  
Data are presented as mean ± S.E.M.; *n* = 3.

Receptor	$[^3\text{H}]\text{DAMGO}$		$[^3\text{H}]\text{U69593}$		$[^3\text{H}]\text{Diprenorphine}$	
	$B_{\text{max}}$	$K_{\text{d}}$	$B_{\text{max}}$	$K_{\text{d}}$	$B_{\text{max}}$	$K_{\text{d}}$
	<i>fmol/mg</i>	<i>nM</i>	<i>fmol/mg</i>	<i>nM</i>	<i>fmol/mg</i>	<i>nM</i>
MOR	263 ± 16	2.9 ± 0.5	N.D.	N.D.	1035 ± 130	0.3 ± 0.1
KOR	N.D.	N.D.	1023 ± 140	6.8 ± 1.8	1465 ± 177	0.3 ± 0.1
MOR-KOR	774 ± 181	17 ± 6**	1235 ± 81	3.0 ± 0.5	2915 ± 230	0.5 ± 0.1

\*\* $P < 0.01$ ,  $t$  test; compared with MOR.

TABLE 5

EC<sub>50</sub> values of different opioid agonists in stimulation of [<sup>35</sup>S]GTPγS binding in membranes from MOR and KOR singly expressing or MOR-KOR coexpressing cells as well as in mixtures of MOR and KOR membranes (MOR + KOR)

Data are mean ± S.E.M.; n = 3. E<sub>max</sub> values did not differ significantly among different membrane preparations.

Compound	MOR-KOR	MOR + KOR	MOR	KOR
	nM			
DAMGO	268 ± 65*	68 ± 8	77 ± 8	2438 ± 65
Endomorphin-1	377 ± 73*	108 ± 8	134 ± 19	2872 ± 128
U69593	0.5 ± 0.1	1.6 ± 1	>1000	1.0 ± 1
U58488H	1.5 ± 1	2.8 ± 1	>1000	1.9 ± 1
GR89696	6 ± 1 fM	4 ± 1 fM	>1	4 ± 1 fM
Morphine	122 ± 7	232 ± 7	187 ± 43	160 ± 10
Dynorphin A1-13	2.8 ± 1	11 ± 1	287 ± 63	1.8 ± 1.3
Etorphine	0.9 ± 0.1	1.2 ± 1.2	0.2 ± 0.3	0.9 ± 0.1
Bremazocine	0.2 ± 0.1	0.1 ± 0.2	0.1 ± 0.3	0.1 ± 0.1

\* P < 0.05, analysis of variance with Dunnett's post test; compared with MOR and MOR + KOR.

multiple functional KOR subtypes (Pesce et al., 1990; Fowler and Fraser, 1994; Kuzmin et al., 2000). MOR and KOR may functionally interact (Suzuki et al., 2001; Narita et al., 2003), potentially generating apparent KOR subtypes. For example, KOR<sub>2</sub> is characterized by residual [<sup>3</sup>H]bremazocine binding in the presence of typical MOR, DOR, and KOR ligands (e.g., DAMGO, [D-Pen<sup>2</sup>, D-Pen<sup>5</sup>]-enkephalin, and U69593 or CI-977) (Fowler and Fraser, 1994). DOR-KOR heterodimer has been linked to the KOR<sub>2</sub> subtype (Jordan and Devi, 1999). On the other hand, KOR<sub>2</sub> could arise from a complex between MOR and KOR, because KOR<sub>2</sub> is absent in MOR-deficient mouse brain (Simonin et al., 2001). Yet, in our study, bremazocine-induced GTPγS binding in MOR-KOR coexpressing cell membranes did not differ between KOR and MOR singly expressing cell-membranes (Table 5). Likewise, GR89696 has been labeled a putative KOR<sub>2</sub> subtype-specific agonist with antihyperalgesic effect (Ho et al., 1997); yet, our ligand binding and GTPγS binding studies (Tables 3 and 5) did not show a substantial difference between KOR homodimer and MOR-KOR heterodimer (Table 4). KOR homodimer and MOR-KOR heterodimer could have different signaling pathways that cannot be differentiated by ligand binding and G protein-coupling assays, as suggested by Childers et al. (1998). Most studies regarding specific effects of GR89696 as a KOR<sub>2</sub> agonist were performed in vivo or in brain slices (Caudle et al., 1997; Ho et al., 1997; Eliav et al., 1999), raising the possibility that the MOR-KOR heterodimer is unstable in membrane preparations or is coupled differently in native tissue.

Whether MOR-KOR heterodimers traffic similar to their respective monomers remains to be determined. The GFP<sup>2</sup> tag was less sensitive for immunofluorescence confocal microscopy, making it difficult to localize the heterodimer. We cannot exclude the possibility that the MOR-KOR dimers are sequestered in some manner so as to make them inaccessible to certain ligand. Therefore, the cellular function of potential MOR-KOR dimers remains to be clarified.

In conclusion, we have used quantitative BRET analysis to assess the relative affinity and the state of opioid receptors interactions. Our results unexpectedly demonstrate that all opioid receptors can form homo- and heterodimers among each other with similar avidity. These results confirm and extend previous results showing opioid receptor oligomerization, and provide a quantitative basis for assessing receptor-receptor interactions. Future studies will focus on the physiological consequences of opioid receptor homo- and heterodimerization.

## References

- Angers S, Salahpour A, Joly E, Hilairat S, Chelsky D, Dennis M, and Bouvier M (2000) Detection of beta 2-adrenergic receptor dimerization in living cells using bioluminescence resonance energy transfer (BRET). *Proc Natl Acad Sci USA* **97**:3684–3689.
- Ayoub MA, Couturier C, Lucas-Meunier E, Angers S, Fossier P, Bouvier M, and Jockers R (2002) Monitoring of ligand-independent dimerization and ligand-induced conformational changes of melatonin receptors in living cells by bioluminescence resonance energy transfer. *J Biol Chem* **277**:21522–21528.
- Bouvier M (2001) Oligomerization of G-protein-coupled transmitter receptors. *Nat Rev Neurosci* **2**:274–286.
- Caudle RM, Mannes AJ, and Iadarola MJ (1997) GR89,696 is a κ-2 opioid receptor agonist and a κ-1 opioid receptor antagonist in the guinea pig hippocampus. *J Pharmacol Exp Ther* **283**:1342–1349.
- Chabre M, Cone R, and Saibil H (2003) Biophysics: is rhodopsin dimeric in native retinal rods? *Nature (Lond)* **426**:30–31; discussion 31.
- Childers SR, Xiao R, Vogt L, and Sim LJ (1998) Lack of evidence of kappa2-selective activation of G-proteins: kappa opioid receptor stimulation of [<sup>35</sup>S]GTPγS binding in guinea pig brain. *Biochem Pharmacol* **56**:113–120.
- Cvejic S and Devi LA (1997) Dimerization of the α opioid receptor: implication for a role in receptor internalization. *J Biol Chem* **272**:26959–26964.
- Eliav E, Herzberg U, and Caudle RM (1999) The kappa opioid agonist GR89,696 blocks hyperalgesia and allodynia in rat models of peripheral neuritis and neuropathy. *Pain* **79**:255–264.
- Filizola M, Olmea O, and Weinstein H (2002) Prediction of heterodimerization interfaces of G-protein coupled receptors with a new subtractive correlated mutation method. *Protein Eng* **15**:881–885.
- Filizola M and Weinstein H (2002) Structural models for dimerization of G-protein coupled receptors: the opioid receptor homodimers. *Biopolymers* **66**:317–325.
- Fotiadi D, Liang Y, Filipek S, Saperstein DA, Engel A, and Palczewski K (2003) Atomic-force microscopy: rhodopsin dimers in native disc membranes. *Nature (Lond)* **421**:127–128.
- Fowler CJ and Fraser GL (1994) μ-, δ-, κ-Opioid receptors and their subtypes. A critical review with emphasis on radioligand binding experiments. *Neurochem Int* **24**:401–426.
- George SR, Fan T, Xie Z, Tse R, Tam V, Varghese G, and O'Dowd BF (2000) Oligomerization of μ- and δ-opioid receptors. Generation of novel functional properties. *J Biol Chem* **275**:26128–26135.
- George SR, O'Dowd BF, and Lee SP (2002) G-protein-coupled receptor oligomerization and its potential for drug discovery. *Nat Rev Drug Discov* **1**:808–820.
- Gomes I, Gupta A, Filipovska J, Szeto HH, Pintar JE, and Devi LA (2004) A role for heterodimerization of μ and delta opioid receptors in enhancing morphine analgesia. *Proc Natl Acad Sci USA* **101**:5135–5139.
- Gomes I, Jordan BA, Gupta A, Trapaidze N, Nagy V, and Devi LA (2000) Heterodimerization of μ and delta opioid receptors: a role in opiate synergy. *J Neurosci* **20**:RC110.
- He L, Fong J, von Zastrow M, and Whistler JL (2002) Regulation of opioid receptor trafficking and morphine tolerance by receptor oligomerization. *Cell* **108**:271–282.
- Hebert TE, Moffett S, Morello JP, Loisel TP, Bichet DG, Barret C, and Bouvier M (1996) A peptide derived from a β2-adrenergic receptor transmembrane domain inhibits both receptor dimerization and activation. *J Biol Chem* **271**:16384–16392.
- Ho J, Mannes AJ, Dubner R, and Caudle RM (1997) Putative κ-2 opioid agonists are antihyperalgesic in a rat model of inflammation. *J Pharmacol Exp Ther* **281**:136–141.
- Issafras H, Angers S, Bulenger S, Blanpain C, Parmentier M, Labbe-Jullie C, Bouvier M, and Marullo S (2002) Constitutive agonist-independent CCR5 oligomerization and antibody-mediated clustering occurring at physiological levels of receptors. *J Biol Chem* **277**:34666–34673.
- Ji RR, Zhang Q, Law PY, Low HH, Elde R, and Hokfelt T (1995) Expression of μ-, δ- and kappa-opioid receptor-like immunoreactivities in rat dorsal root ganglia after carrageenan-induced inflammation. *J Neurosci* **15**:8156–8166.
- Jordan BA and Devi LA (1999) G-protein-coupled receptor heterodimerization modulates receptor function. *Nature (Lond)* **399**:697–700.
- Kuzmin A, Sandin J, Terenius L, and Ogren SO (2000) Dose- and time-dependent bimodal effects of κ-opioid agonists on locomotor activity in mice. *J Pharmacol Exp Ther* **295**:1031–1042.
- Lavoie C, Mercier JF, Salahpour A, Umaphathy D, Breit A, Villeneuve LR, Zhu WZ, Xiao RP, Lakatta EG, Bouvier M, et al. (2002) β1/β2-Adrenergic receptor het-



- erodimerization regulates  $\beta$ 2-adrenergic receptor internalization and ERK signaling efficacy. *J Biol Chem* **277**:35402–35410.
- McVey M, Ramsay D, Kellett E, Rees S, Wilson S, Pope AJ, and Milligan G (2001) Monitoring receptor oligomerization using time-resolved fluorescence resonance energy transfer and bioluminescence resonance energy transfer. The human delta-opioid receptor displays constitutive oligomerization at the cell surface, which is not regulated by receptor occupancy. *J Biol Chem* **276**:14092–14099.
- Mercier JF, Salahpour A, Angers S, Breit A, and Bouvier M (2002) Quantitative assessment of beta 1- and beta 2-adrenergic receptor homo- and heterodimerization by bioluminescence resonance energy transfer. *J Biol Chem* **277**:44925–44931.
- Morinville A, Cahill CM, Esdaile MJ, Aibak H, Collier B, Kieffer BL, and Beaudet A (2003) Regulation of delta-opioid receptor trafficking via mu-opioid receptor stimulation: evidence from mu-opioid receptor knock-out mice. *J Neurosci* **23**:4888–4898.
- Narita M, Khotib J, Mizoguchi H, Suzuki M, Ozaki S, Yajima Y, Tseng LF, and Suzuki T (2003) Direct evidence for the up-regulation of spinal micro-opioid receptor function after repeated stimulation of kappa-opioid receptors in the mouse. *Eur J Neurosci* **18**:2498–2504.
- Overton MC and Blumer KJ (2000) G-protein-coupled receptors function as oligomers in vivo. *Curr Biol* **10**:341–344.
- Park PS and Wells JW (2003) Monomers and oligomers of the M2 muscarinic cholinergic receptor purified from Sf9 cells. *Biochemistry* **42**:12960–12971.
- Pesce GO, Cruciani RA, Munson PJ, and Rodbard D (1990) Computer modeling of subtypes of kappa opioid receptors in adrenal medulla. *Eur J Pharmacol* **182**:429–439.
- Pfeiffer M, Koch T, Schroder H, Klutzny M, Kirsch S, Kreienkamp HJ, Holtt V, and Schulz S (2001) Homo- and heterodimerization of somatostatin receptor subtypes. Inactivation of sst(3) receptor function by heterodimerization with sst(2A). *J Biol Chem* **276**:14027–14036.
- Ramsay D, Kellett E, McVey M, Rees S, and Milligan G (2002) Homo- and hetero-oligomeric interactions between G-protein-coupled receptors in living cells monitored by two variants of bioluminescence resonance energy transfer (BRET): hetero-oligomers between receptor subtypes form more efficiently than between less closely related sequences. *Biochem J* **365**:429–440.
- Raser JM and O'Shea EK (2004) Control of stochasticity in eukaryotic gene expression. *Science (Wash DC)* **304**:1811–1814.
- Salahpour A, Angers S, Mercier JF, Lagace M, Marullo S, and Bouvier M (2004) Homodimerization of the  $\beta$ 2-adrenergic receptor as a prerequisite for cell surface targeting. *J Biol Chem* **279**:33390–33397.
- Schneider D, Liu Y, Gerstein M, and Engelman DM (2002) Thermostability of membrane protein helix-helix interaction elucidated by statistical analysis. *FEBS Lett* **532**:231–236.
- Shaquira MA, Zollner C, Mousa SA, Stein C, and Schafer M (2004) Characterization of  $\mu$  opioid receptor binding and G protein coupling in rat hypothalamus, spinal cord and primary afferent neurons during inflammatory pain. *J Pharmacol Exp Ther* **308**:712–718.
- Simonin F, Slowe S, Becker JA, Matthes HW, Filliol D, Chluba J, Kitchen I, and Kieffer BL (2001) Analysis of [ $^3$ H]bremazocine binding in single and combinatorial opioid receptor knockout mice. *Eur J Pharmacol* **414**:189–195.
- Suzuki S, Chuang LF, Doi RH, Bidlack JM, and Chuang RY (2001) kappa-Opioid receptors on lymphocytes of a human lymphocytic cell line: morphine-induced up-regulation as evidenced by competitive RT-PCR and indirect immunofluorescence. *Int Immunopharmacol* **1**:1733–1742.
- Terrillon S, Durroux T, Mouillac B, Breit A, Ayoub MA, Taulan M, Jockers R, Barberis C, and Bouvier M (2003) Oxytocin and vasopressin V1a and V2 receptors form constitutive homo- and heterodimers during biosynthesis. *Mol Endocrinol* **17**:677–691.
- Tucker CL, Gera JF, and Uetz P (2001) Towards an understanding of complex protein networks. *Trends Cell Biol* **11**:102–106.
- Zhao GM, Qian X, Schiller PW, and Szeto HH (2003) Comparison of [Dmt1]DALDA and DAMGO in binding and G protein activation at  $\mu$ ,  $\delta$  and  $\kappa$  opioid receptors. *J Pharmacol Exp Ther* **307**:947–954.

---

**Address correspondence to:** Dr. Wolfgang Sadée, Department of Pharmacology, School of Medicine and Public Health, The Ohio State University, Columbus, OH 43210. E-mail: sadee.1@osu.edu

---